Studies on Wake-Affected Heat Transfer Around the Circular Leading Edge of Blunt Body

K. Funazaki
Department of Mechanical Engineering,
Iwate University,
Morioka, Iwate, Japan

Detailed measurements are performed about time-averaged heat transfer distributions around the leading edge of a blunt body, which is affected by incoming periodic wakes from the upstream moving bars. The blunt body is a test model of a front portion of a turbine blade in gas turbines and consists of a semicircular cylindrical leading edge and a flat plate afterbody. A wide range of the steady and unsteady flow conditions are adopted as for the Reynolds number based on the diameter of the leading edge and the bar-passing Strouhal number. The measured heat transfer distributions indicate that the wakes passing over the leading edge cause a significant increase in heat transfer before the separation and the higher Strouhal number results in higher heat transfer. From this experiment, a correlation for the heat transfer enhancement around the leading edge due to the periodic wakes is deduced as a function of the Stanton number and it is reviewed by comparison with the other experimental works.

Introduction

Due to demands for more efficient and powerful aeroengines or gas turbines, turbine inlet temperature (TIT) has been constantly increasing during the last decade, and will become higher than 1800 K in the near future, as pointed out by Yoshida (1993). This high TIT can be attained by efficient blade cooling technologies as well as development of new materials for turbine blades. As for the blade cooling, an accurate prediction of a heat transfer distribution along the blade surface is indispensable and many efforts have been devoted to develop reliable prediction methods. They are based on, for example, rather simple correlations, boundary layer analyses with a turbulent model, or solvers of Navier–Stokes equations. Not a few efforts are directed to studies of turbine blade leading edge problems because the heat load around the leading edge where the flow stagnates is intrinsically very large; furthermore, incident mainstream turbulence increases the heat load to great extent. Frossling (1958) proposed an empirical correlation for the heat transfer distribution around the leading edge, $\mathrm{Nu}_D(\theta)$, such as

$$\frac{\mathrm{Nu}_D(\theta)}{\mathrm{Re}_D^{1/2}} = 0.9449 - \frac{0.510}{4}\theta^2 - \frac{0.596}{16}\theta^4, \qquad (1)$$

where θ is an angle from the stagnation line; Re_D is Reynolds number based on the inlet velocity and the diameter of the leading edge. On the other hand, Lowry and Vachon (1975) showed the following equation for the stagnant heat transfer, $\mathrm{Nu}_{D,\max}$:

$$\frac{\mathrm{Nu}_{D,\max}}{\mathrm{Re}_D^{1/2}} = 1.01 + 2.624\left[\frac{Tu\ \mathrm{Re}_D^{1/2}}{100}\right] - 3.07\left[\frac{Tu\ \mathrm{Re}_D^{1/2}}{100}\right]^2, \qquad (2)$$

where Tu is a mainstream turbulence intensity.

Recently, effects of wake–blade interaction upon the heat transfer not only around the stagnation region of the leading edge but also on the blade surface have been collecting attention from a large number of researchers. Magari and LaGraff (1994) measured heat transfer distributions around the stagnation region of a circular cylinder that was immersed inside the wake from a stationary cylinder with smaller diameter, and found the importance of large vortical structures shed from the upstream cylinder (wake generator) in the heat transfer process around the leading edge. Likewise O'Brien (1990) conducted the measurement of the heat transfer distributions around the stagnation region of a circular cylinder that was under the influence of wake-passing generated from the upstream moving bars. He found an asymmetric heat transfer distribution about the geometrically determined stagnation line, especially at higher Strouhal number cases. Paxson and Mayle (1991), on the other hand, conducted unsteady velocity measurements of wake-affected laminar boundary layers around the stagnation region of a rounded bluff body, which can be regarded as a more appropriate model of a turbine blade than a circular cylinder. They discussed the validity of a perturbation approach to describe the unsteady disturbed flow. Furthermore, Dullenkopf and Mayle (1994) examined the effect of free-stream turbulence on augmenting heat transfer in accelerating flow regions such as a leading edge or aft portion of a turbine blade, and proposed a correlation that could fit with the experimental data as follows:

$$\mathrm{Nu}_a\ \mathrm{Pr}^{-0.37} = 0.571 + 0.0125 Tu_a\left\{1 + \frac{2}{1 + (Tu_a/25)^3}\right\},$$

$$\mathrm{Nu}_a = \mathrm{Nu}_c/\sqrt{a_1\ \mathrm{Re}_c},\ Tu_a = Tu\sqrt{\mathrm{Re}_c/a_1} \qquad (3)$$

where Nu_a is a local Nusselt number based on the blade chord length and a_1 is a coefficient of constant flow acceleration. They claimed that the above-mentioned correlation was able to apply to the prediction of the effect of periodically passing wakes on the heat transfer over the pressure surface of a turbine blade.

In this study, using a blunt test model with a semicircular leading edge similar to that of Mehendale et al. (1991) and a wake generator consisting of moving cylinders, detailed experiments are made to measure the influence of the periodically passing wakes on the heat transfer distribution over the surface. Much focus of the study is placed upon the wake effects on the

Contributed by the International Gas Turbine Institute and presented at the 39th International Gas Turbine and Aeroengine Congress and Exposition, The Hague, The Netherlands, June 13–16, 1994. Manuscript received by the International Gas Turbine Institute February 4, 1996. Paper No. 94-GT-25. Associate Technical Editor: E. M. Greitzer.

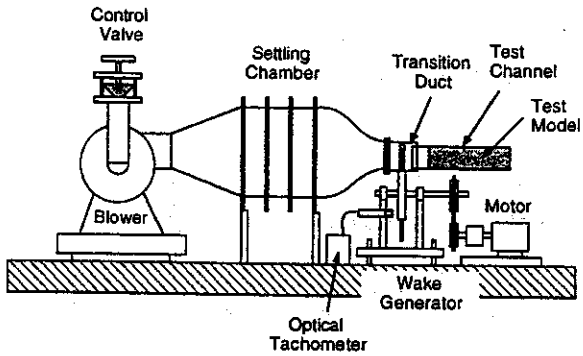

Fig. 1 Schematic layout of the test apparatus

heat transfer augmentation at the stagnation region, as well as upon the wake-induced peak value variations of the heat transfer at the reattachment point.

Test Apparatus

Outline. A schematic layout of the test apparatus is shown in Fig. 1. Air from the blower is led to contraction nozzle with the exit cross section of 240 mm × 350 mm, passing through the settling chamber. Flow rate is adjusted by the inlet valve of the blower. The acrylic resin transition duct attached to the nozzle has a slot through which circular cylinders on the rim of the rotating disk can move, generating wakes behind them. The front portion of the test channel containing the test model is inserted into the transition duct, removing the upstream boundary layer as a result of the transition duct, so that the boundary layer inside the test channel starts from the leading edge of the test channel.

Wake Generator. Six circular cylinders of 5 mm diameter and 250 mm length can be mounted on the disk rim. Since the disk is made of brass and its diameter is 400 mm, its inertia is large enough to maintain a nearly constant rotational speed. The rotational speed of the disk is controlled by the transmission gear box connected to the induction motor and it is monitored by an optical tachometer or a stroboscope. The range of rotational speed is 900–1500 rpm. A slight vibration of the cylinder probably due to the flow and the structural vibration was observed but it didn't seem to alter the wake characteristics drastically.

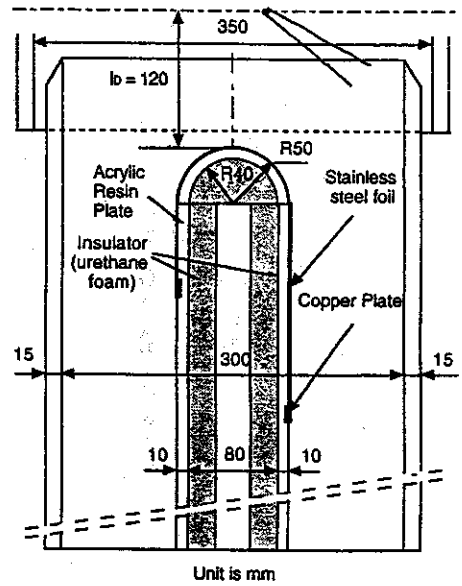

Fig. 2 Test model for heat transfer measurement

Test Channel. The cross section of the test channel is 200 mm height and 300 mm width and its length is 1000 mm. The front end of the channel is sharp-edged and is inserted into the transition duct with 10 mm clearance around it. On the one side of the test channel, there is a longitudinal slot for the measurement of the inlet velocity by a Pitot tube and incident wakes by a hot-wire probe. This slot is usually plugged with several blocks with great care paid to the air leakage during the test run.

Test Model

Test Model for Heat Transfer Measurement. The test model for the heat transfer measurement has exactly the same geometry with that for the pressure measurement, which is shown in Fig. 2. Along the midspan of the test model, 60 holes are shaped through the cylinder and the plate with equal surface wise distance. Each of the holes is plugged with small piece of urethane

Nomenclature

a_1 = acceleration parameter
C_D = drag coefficient
D = diameter of test model leading edge or drag
d = diameter of circular cylinder
h = heat transfer coefficient
f = wake-passing frequency = $nn_c/60$
l_D = axial distance between the moving bars and the test model
n, n_c = number of rotation, number of circular cylinder
$\mathrm{Nu}_D(x)$ = local Nusselt number based on the leading edge diameter
$\mathrm{Nu}_{D,\max}$ = maximum Nusselt number
p = static pressure
$\dot{q}_{\mathrm{wall}}$, $\dot{q}_{\mathrm{loss}}$ = wall heat flux, heat loss
R = radius of test model leading edge
Re_D = Reynolds number based on the leading edge diameter and inlet flow
Re_x = local Reynolds number = $U(x_{\mathrm{surf}})x_{\mathrm{surf}}/\upsilon$
S = Strouhal number = fD/U_{in}
St = local Stanton number = $\mathrm{Nu}_x/\mathrm{Re}_x\mathrm{Pr}$
t = pitch of wake-generating bars
T_{wall}, T_∞ = wall temperature, inlet flow temperature
Tu = turbulence intensity
U_{in}, $U(x_{\mathrm{surf}})$ = inlet velocity, local velocity along the model surface
W_1, W_2, W_∞ = relative inlet, outlet, and vector-averaged flow velocities
x, x_{surf} = axial length, surface length
β_1, β_2 = relative inlet and outlet flow angles in the frame of the moving bars
$\Delta\beta$ = turning angle
ϵ = emissivity
θ = angle measured from the stagnation point
λ = thermal conductivity
ν = kinematic viscosity
ρ = density
σ = Stefan–Boltzmann constant

Subscripts

0 = values free from the wake effect
1, 2 = inlet, outlet
max = maximum
w = wake-affected values

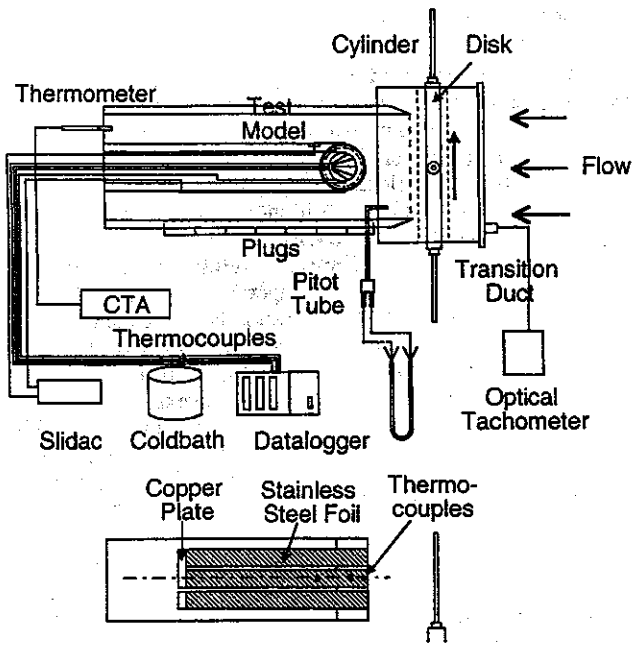

Fig. 3 Schematic of the measurement system

foam and then a hot junction of a K-type thermocouple is flush-mounted on the measurement surface penetrating back through the urethane foam. Lines of the thermocouples are then connected to a computer-controlled datalogger (Data Acquisition Controller, NEC San-ei) to convert the signals to digital ones, where 10 samples for each measuring point are acquired during one scan.

Very thin stainless steel adhesive tapes of 30 mm width and 700 mm length are pasted on the surface of the test model as a heater, one of which covers the hot junctions on the surface. Those tapes are connected through the copper plates in series to form an electric circuit and electric power is supplied to it from a power controller in order to obtain a constant heat flux condition on the measurement surface. To prevent the tapes from buckling due to thermal elongation, they are covered by transparent tapes (3M Booktape 845) of 90 μm thickness. Temperature drop through these tapes is estimated to be about 0.25°C.

Test Model for Pressure Measurement. The test model used for the the pressure measurement has the same geometry as the model of Fig. 2. It consists of a semicircular component and two flat plates, and at the midspan of the model several small holes of 1.1 mm diameter are dug through the plates for the wall static pressure measurement. Very small Teflon tubes are inserted through each of the holes, which are then connected to a Betz type manometer of ±0.49 Pa precision.

Experiments

A schematic of the measurement system is shown in Fig. 3. Setting the inlet velocity to specified values, i.e., 5 m/s, 10 m/s, 15 m/s, and 20 m/s, corresponding to $Re_D = 3.4 \times 10^4$, 6.7×10^4, 10.0×10^4, and 13.3×10^4, respectively, the stainless steel foil on the test model is then heated for two or three hours in order to achieve thermal equilibrium on the test model. After confirmation of the thermal equilibrium condition by monitoring the surface temperature distribution T_{wall}, the surface temperature distribution is measured, which then yields heat transfer coefficient $h(x)$ and Nusselt number Nu_D on the test model as follows:

$$h(x) = \frac{\dot{q}_{wall}}{T_{wall}(x) - T_\infty} = \frac{\dot{q}_{supply} - \dot{q}_{loss}}{T_{wall}(x) - T_\infty} \tag{4}$$

$$Nu_D(x) = \frac{h(x)D}{\lambda}, \tag{5}$$

where heat flux $\dot{q}_{supply}$ is an electrical power supply, $\dot{q}_{loss}$ is heat flux that does not contribute to $\dot{q}_{wall}$ (the convective heat flux from the surface), T_{wall} is an ambient temperature around the test model measured at the downstream of the test channel as seen in Fig. 4. The heat flux, $\dot{q}_{loss}$, consists of radiation heat flux, $\dot{q}_{rad}$, and conduction heat flux inside the plate, $\dot{q}_{cond}$.

Radiation heat flux from the heated surface can be, in principle, evaluated with the Stefan–Boltzmann radiation equation (Benedict, 1969). In such a case precise information about the configuration factor as well as the emissivity of each of the heated surfaces is indispensable. However, such information, especially configuration factor, is not always easily available, so that a simplified approach is taken to assess the configuration factor. On the semicircular cylinder surface, its configuration factor is assumed to be unity, which yields the following expression as for the radiation heat flux around the leading edge of the test model:

$$\dot{q}_{rad} = \sigma\epsilon_1(\overline{T}^4_{wall,1} - T^4_{ambient}), \tag{6}$$

where σ is the Stefan–Boltzmann constant ($=5.67 \times 10^{-8}$ W/($m^2 \cdot K^4$)), ϵ_1 is the emissivity of the stainless steel foil, estimated to be 0.22 according to Mehendale et al. (1991). On the other hand, the radiation heat flux on the flat plate is evaluated using a correlation for parallel infinite plates as follows:

$$\dot{q}_{rad} = \sigma(\overline{T}^4_{wall,1} - T^4_{ambient}) \frac{1}{\frac{1}{\epsilon_1} + \frac{1}{\epsilon_2} - 1}, \tag{7}$$

where ϵ_2 is the emissivity of the acrylic resin plate opposite to the heated stainless steel foil and it is assumed to be 0.9.

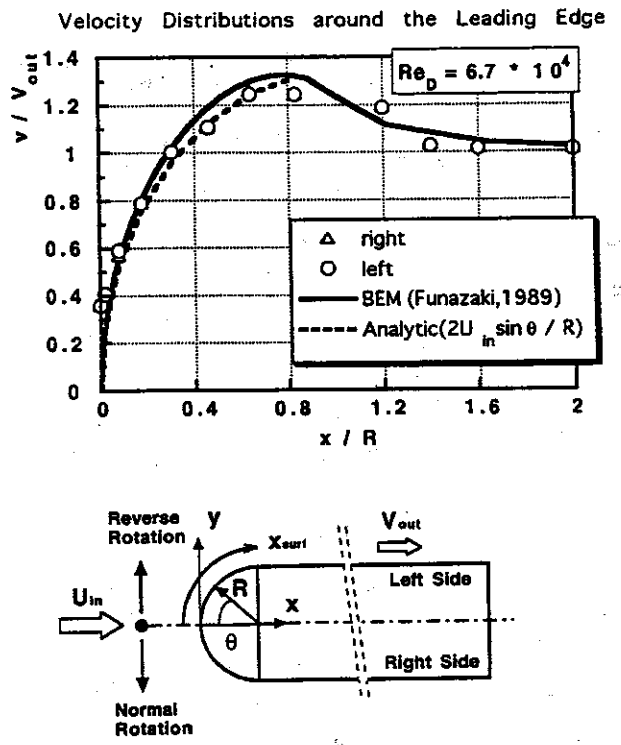

Fig. 4 Velocity distribution measured around the test model, with some incompressible flow calculations, and some notations about the coordinate system of the test model; $Re_D = 6.7 \times 10^4$

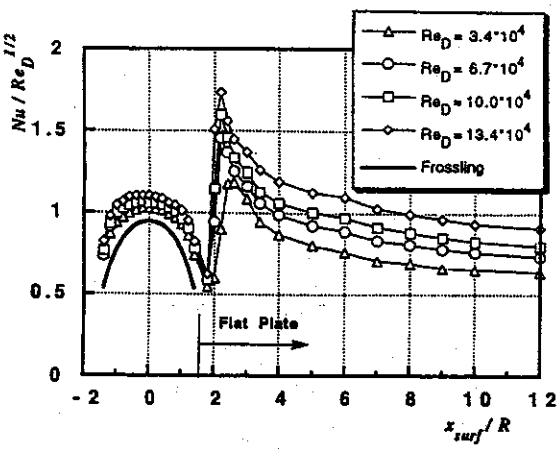

Fig. 5 Heat transfer distributions with no influences of incident wakes, which are represented in terms of the Frossling factor

A preliminary experiment was conducted in order to deduce a correlation for the conduction heat flux, where an averaged surface temperature and an ambient temperature were measured with small level of electric power being applied to the stainless steel foil for at least an hour. Note that a rather parasitic heat flux was inevitable around the copper electrodes due to its contact resistance with the stainless steel foils and it was found to be about 10 percent of the supplied electric power. The contribution of such heat flux to the total conduction heat flux was incorporated in the above-mentioned correlation.

Uncertainty

An uncertainty analysis was carried out using the method of Kline and McClintock (1953). The estimated uncertainties in h, Nu, and Re were 3.5, 4.1, and 3.6 percent, respectively.

Results

Velocity Distribution. The test model is placed at the center of the test channel so as to establish the symmetric flow field with respect to the centerline of the model. Such asymmetry is confirmed by the measurement of the velocity distribution along the model surface, as appeared in Fig. 5. This figure shows the normalized velocity distributions on the right and left sides of the model in the case of $Re_D = 6.7 \times 10^4$, where Re_D is Reynolds number based on the 100 mm diameter of the semicircular cylinder. Note that the right side of the test model when viewed from the inlet of the test channel is referred to as "right" and vice versa. Also shown in Fig. 4 are the calculations of the velocity distribution by BEM (Boundary Element Method) developed by Funazaki (1989) and the analytic solution for a circular cylinder. Measured velocity distributions on both sides of the test model coincide, which verifies the symmetric flow field. The calculations agree with the measured data fairly well, except around the junction between the semicircular cylinder and the flat plates. Close investigation has revealed that this discrepancy can be attributed to a small separation bubble existing around there. As the inlet velocity increases, the differences between the measured data and the calculation become larger and the measured distributions become flatter, which means an advancement of the separation point, i.e., a growth of the separation bubble. It was also identified in an oil-flow visualization.

Heat Transfer Distribution

Heat Transfer in Steady (No-Wake) Flow Conditions. Figure 5 presents local heat transfer distributions for four different cases of the inlet Reynolds number. Also shown in this figure is the curve of Eq. (1).

All these data expressed in terms of $Nu_D/Re_D^{1/2}$ tend to converge onto a single curve along the leading edge with a band of scatter. This scatter is probably due to uncertainty in the data and the effect of the inlet free-stream turbulence, which was about 0.8 percent. The local heat transfer decreases from the stagnation point down to the position just beyond the cylinder-flat plate junction ($x_{surf}/R \cong 1.8$), followed by the rapid increase and then the gradual decrease toward the aft portion of the flat plate. Apparently, such drastic changes in heat transfer around the junction are caused by the separation bubble existing there.

In order to examine an incoming wake effect on the heat transfer distribution over the surfaces of both the circular leading edge and the flat plate, it is convenient to express the distribution in terms of Stanton number against the local Reynolds number, Re_x. Figure 6 illustrates the Stanton number distributions for the no-wake flow conditions versus Re_x along the left surface of the test model. In this figure the following two lines are also plotted:

$$St = 0.57Pr^{-0.6} Re_x^{-0.5}, \quad (8)$$

the laminar solution for the two-dimensional stagnation flow with a linear velocity distribution from the stagnation point, and

$$St = 0.0307Pr^{-0.4} Re_x^{-0.2}, \quad (9)$$

a turbulent flow correlation over the flat plate given by Kays and Crawford (1980). The heat transfer data before the abrupt change in Stanton number in Fig. 6 follow the line of Eq. (8) very well for all cases of the inlet flow conditions. After the maximum points of the Stanton number, which correspond to the reattachment points, the data gradually follow the line of Eq. (9) for the turbulent flow correlation.

Wake-Affected Heat Transfer. Figure 7 shows wake-affected heat transfer distributions on the test model for the lowest Reynolds number case among the test conditions ($Re_D = 3.4 \times 10^4$). Unsteady flow parameter adopted here is a bar-passing Strouhal number, S, defined as

$$S = \frac{fD}{U_{in}}, \quad (10)$$

$$f = \frac{nn_c}{60}, \quad (11)$$

where n is a rotational speed of the wake generator, n_c is the number of the cylinders attached to it, and D is the diameter of the leading edge of the test model. Compared to the heat transfer

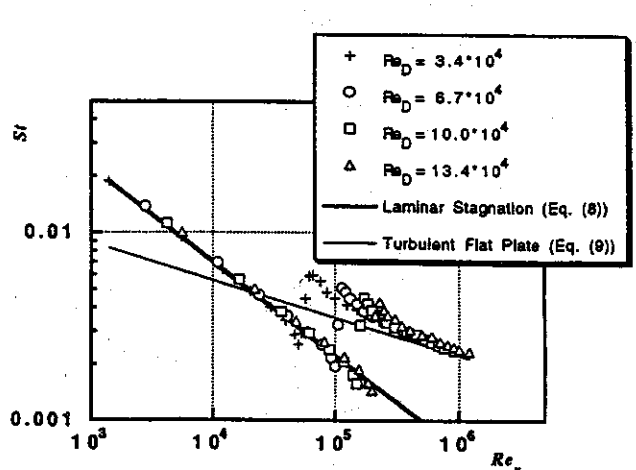

Fig. 6 Stanton number distributions against local Reynolds number under no-wake conditions

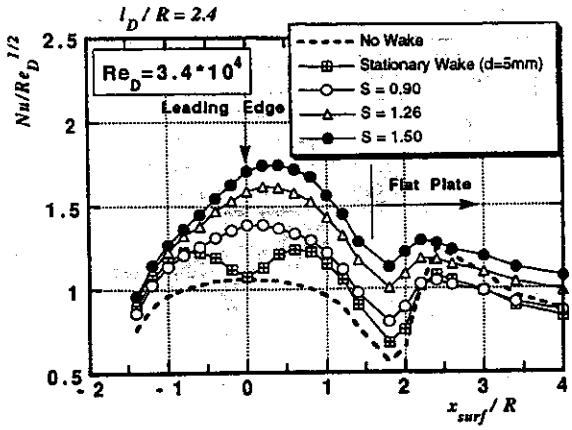

Fig. 7 Wake-affected heat transfer distributions on the test model for several unsteady flow conditions; $Re_D = 3.4 \times 10^4$

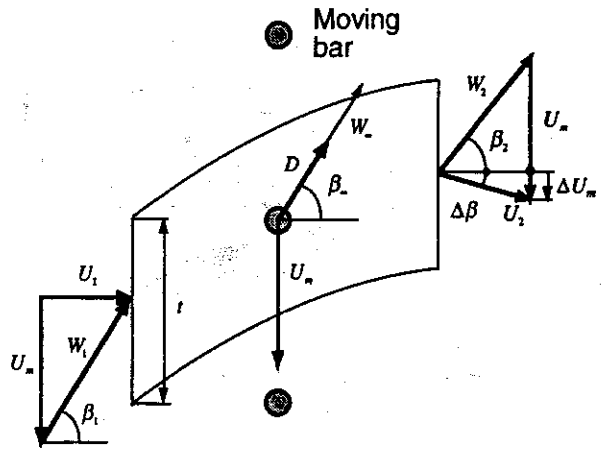

Fig. 9 The moving bars and the inlet/outlet velocity diagrams

data in the no-wake condition, overall levels of the heat transfer around the leading edge as well as on the flat plate increase considerably as the Strouhal number increases. Investigation into the data has revealed that the profiles of the heat transfer distributions along the leading edge are asymmetric with respect to the centerline of the test model and the peak positions shift toward the "left" side of the model. To inspect the mechanism of this phenomenon, additional experiments were conducted by rotating the wake generator in reverse, which results in the data of Fig. 8. It is very clear that the peak positions tend to move toward the "right" side of the model due to the reverse rotation, while the profiles of both cases are apparently a mirror image relationship. One of the possible explanations for the phenomenon is that the movement of the cylinders causes the flow to turn, which leads to nonzero incident angle of the inlet flow to the test model and consequently results in the shift of the actual stagnation line from the geometric one. Such supposition can be easily verified by applying the two-dimensional cascade theory to the present case as shown in Fig. 9. Note that the control volume of Fig. 9 has an unit depth of the cylinder. It follows that the flow turning angle measured from the geometric stagnation line, $\Delta\beta$, is given by

$$\Delta\beta = \tan^{-1}\frac{\Delta U_m}{U_1} \tag{12}$$

$$\Delta U_m = W_2 \sin\beta_2 - W_1 \sin\beta_1 = \frac{D\sin\beta_\infty}{\rho t W_\infty \cos\beta_\infty \cdot 1} \cong \frac{D\sin\beta_1}{\rho t U_1}, \tag{13}$$

$$t = \frac{2\pi R}{n_c},\ D = C_D d\frac{\rho}{2}W_\infty^2 \cong C_D d\frac{\rho}{2}W_1^2 \tag{14}$$

The results are plotted in Fig. 10. This shows that the positions of the calculated stagnation line and the measured heat transfer peak positions coincide fairly well. It should be noted that the minimum values of the heat transfer data as well as the overall heat transfer levels after the separation are quite different between the normal and reverse rotation cases, probably because the growth rates of the boundary layers for those cases are significantly different.

Additional heat transfer data referred to as "Stationary Wake" are also plotted in Fig. 7. These were obtained by setting one of the circular cylinders on the wake generator just in front of the leading edge of the test model so that the wake from that cylinder constantly covered the surface of the test model. Twin peaks of the heat transfer appear at almost symmetric positions about $x_{surf}/R = 0.0$ at which the minimum heat transfer is identified. These peaks can be attributed to the shear layers of the wake that impact upon the surface of the model front portion. Figure 11 expressed in a logarithmic form in Fig. 6, presents the curves of the wake-affected Stanton number distributions against the local Reynolds number. The Stanton number distribution before the separation bubble increases according to the Strouhal number as in the no-wake condition, being in a linear relation with respect to Nu_x in this diagram. Keep in mind that the data for the no-wake conditions are in good agreement with the correlation for the laminar stagnation flow (Eq. (8)). After

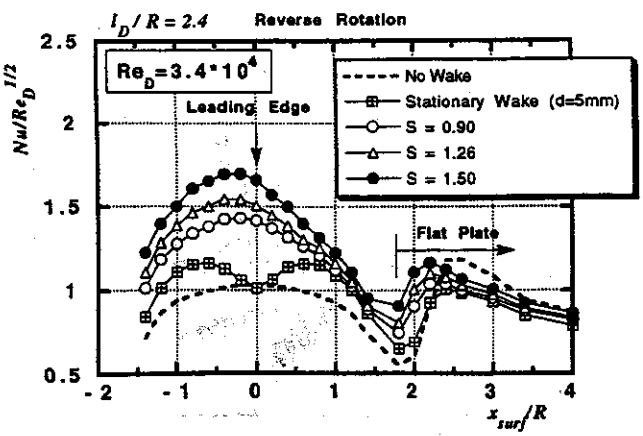

Fig. 8 Wake-affected heat transfer distributions on the test model obtained with the wake generator being rotated in reverse, while other flow conditions are the same with Fig. 7

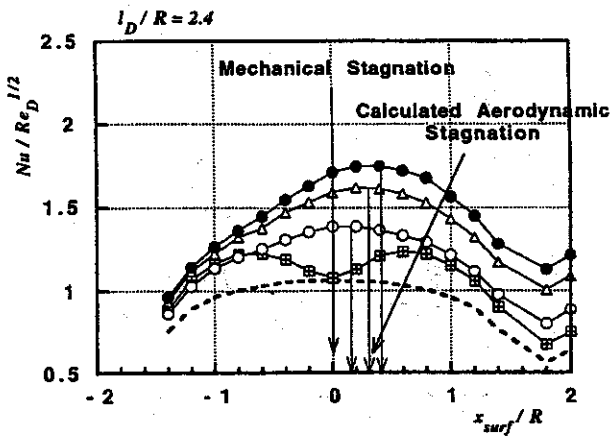

Fig. 10 Shift of the aerodynamic stagnation line due to the moving wake-generating bars; experimental data and predictions by the two-dimensional cascade theory

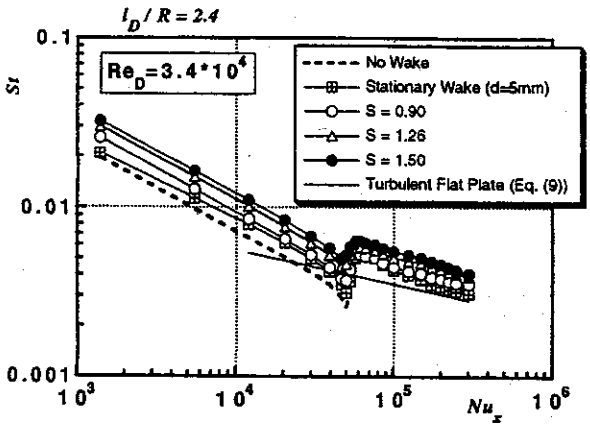

Fig. 11 Wake-affected Stanton number distributions against local Reynolds number; $Re_D = 3.4 \times 10^4$

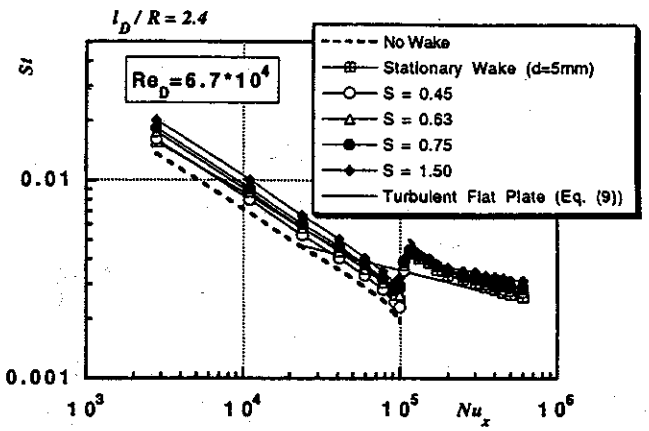

Fig. 13 Wake-affected Stanton number distributions against local Reynolds number; $Re_D = 6.7 \times 10^4$

the reattachment, the Stanton number distributions under the unsteady flow conditions look like those of the turbulent flow but the differences between the data and the correlation (Eq. (9)) are relatively large, while the heat transfer data for the stationary wake case tend to follow the correlation. These phenomena can also be attributed to the shift of the actual stagnation lines.

As the inlet Reynolds number increases, the profiles of the wake-affected heat transfer distributions around the semi-circular cylinder become almost symmetric about $x_{surf}/R = 0.0$, as illustrated in Fig. 12. This is expected from Eq. (10), that is, even at the highest Strouhal number in this case ($S = 1.5$) the calculation yields the stagnation position to be $x_{surf}/R = 0.22$, which almost corresponds to the measured peak position for the same condition. Likewise in the previous case, heat transfer along the test model surface is considerably enhanced due to the increase in the Strouhal number; Fig. 13 also confirms this situation. In this case the Stanton number after the reattachments is likely to follow the correlation for the turbulent flow, although slight deviations appear with the Strouhal number.

Both Figs. 14 and 15 show the case for the highest inlet Reynolds number among the present experiments. In this case the moving wake effect on the heat transfer distribution is seen to be like the previous cases, but the data under the influence of the stationary wake show some pronounced increase in their overall level compared to the data in Fig. 8 or Fig. 12. After the reattachment, on the other hand, the heat transfer data for the entire Strouhal numbers differ very little from one another.

In these observations, the distance between the rotation plane of the bars and the leading edge of the test model, l_D, was fixed to be $l_D/R = 2.4$. In order to examine an effect of such distance on the wake-affected heat transfer, the test model was moved downward by 100 mm so that l_D/R be 4.4, in which case it was expected that the extended distance could alter the wake characteristics. Figure 16 reveals the results for that case. Compared with the previous results in Fig. 14, one might notice that the minimum value of the heat transfer at the stagnation line

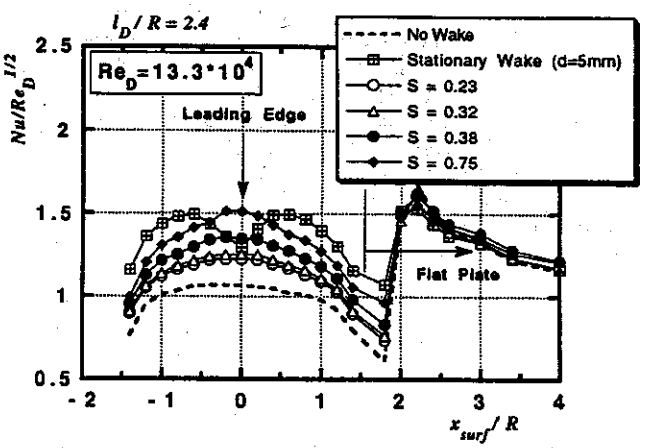

Fig. 14 Wake-affected heat transfer distributions on the test model for several unsteady flow conditions; $Re_D = 13.3 \times 10^4$

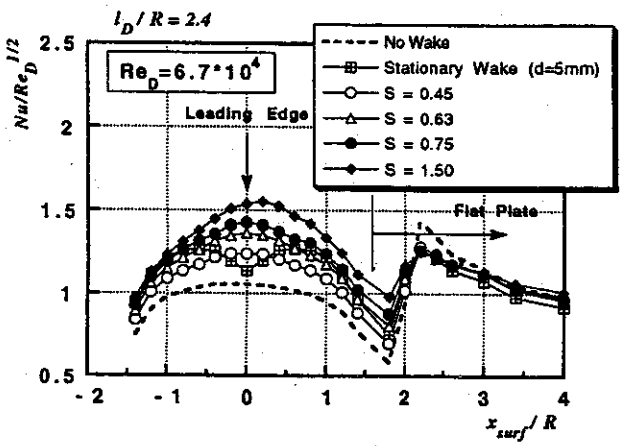

Fig. 12 Wake-affected heat transfer distributions on the test model for several unsteady flow conditions; $Re_D = 6.7 \times 10^4$

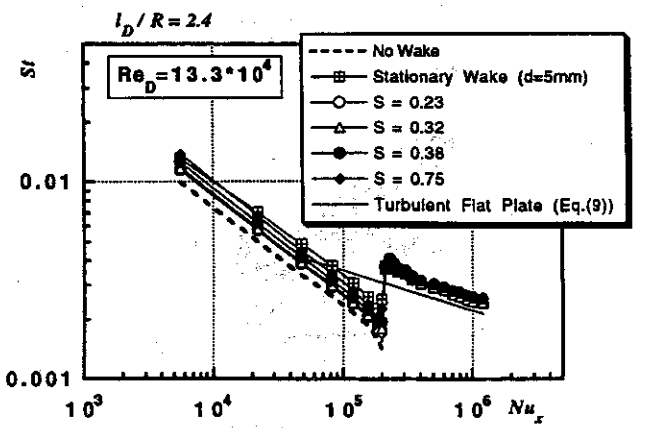

Fig. 15 Wake-affected Stanton number distributions against local Reynolds number; $Re_D = 13.3 \times 10^4$

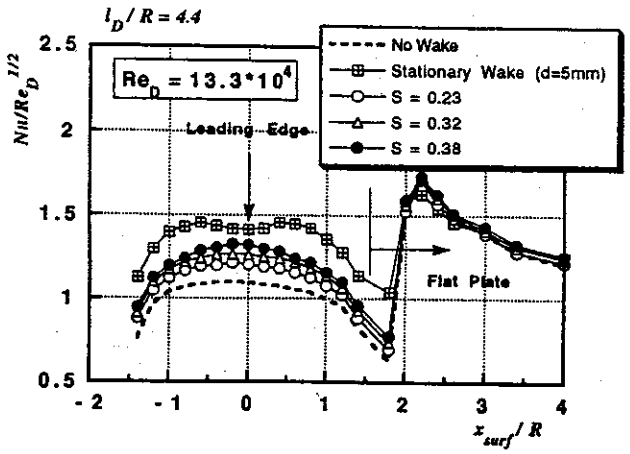

Fig. 16 Wake-affected heat transfer distributions on the test model with the distance between the bars and the test model being elongated; $l_D/R = 4.4$, $Re_D = 13.3 \times 10^4$

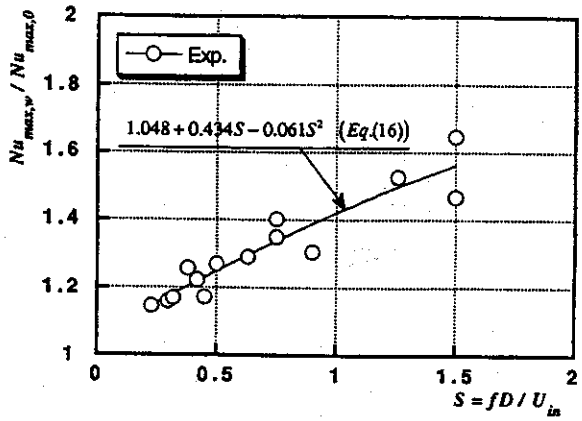

Fig. 18 Dependency of the maximum wake-affected Nusselt numbers on the bar-passing Strouhal number and its correlation

increases at the stationary wake condition and the protruding twin peaks identified in Fig. 14 almost disappear. This is obviously due to the decay of the shear layers in the wake. On the contrary, the heat transfer distributions at the unsteady flow conditions show very little change.

From those observations mentioned above, it appears that the wakes from the moving cylinders enhance the heat transfer around the leading edge of the test model to a great extent, the dependency of the Stanton number on the local Reynolds number being almost unchanged. Therefore the wake-affected heat transfer of the stagnant flow around the leading edge can be expressed from an analogy with Eq. (8) as follows:

$$\overline{St}_w = C\ Pr^{-0.6}\ Re_x^{-0.5} \tag{14}$$

where C is a proportional factor, which could be a function of Strouhal number, incident wake characteristics, inlet Reynolds number, and so on. It seems natural to assume that the Strouhal number is a dominant parameter in the heat transfer enhancement, so that by calculating $\overline{St}_w/Pr^{-0.6}\ Re_x^{-0.5}$ from the heat transfer data before the separation bubble, and then interpolating such results by a polynomial function of the Stanton number, the following expression for the factor C can be deduced, as shown in Fig. 17:

$$C(S) = 0.626 + 0.162S + 0.016S^2 \tag{15}$$

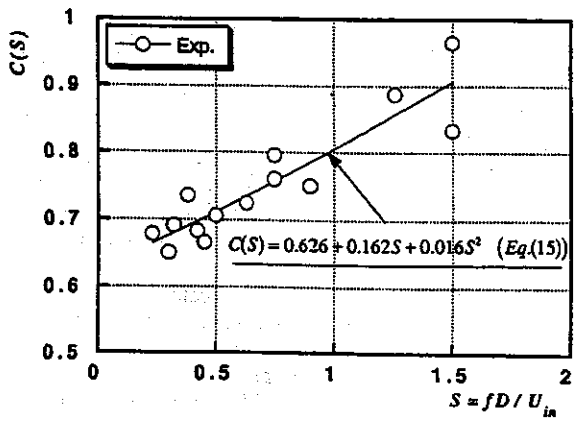

Fig. 17 Correlation for the enhancement factor of the wake-affected heat transfer averaged around the leading edge, which is a function of the bar-passing Strouhal number

Despite some data scattering, Fig. 18 as well as the interpolated expression Eq. (15) reveal the clear dependency of the heat transfer enhancement around the leading edge upon the Strouhal number, which is rather in contrast to the case for the Stanton number after the reattachment.

Strictly speaking, Eq. (15) cannot hold on the stagnation line because of the definition of Stanton number. Hence, for the convenience of a later discussion, a correlation for heat transfer enhancement on the stagnation line, $Nu_{max,w}/Nu_{max,0}$, shown in Fig. 18, is given as

$$\frac{Nu_{max,w}}{Nu_{max,0}} = 1.048 + 0.434S - 0.061S^2. \tag{16}$$

It should be noted that the dependencies of $C(S)$ and $Nu_{max,w}/Nu_{max,0}$ on the Strouhal number are not the same. This is because, in contrast to the case of Fig. 18, each of the points in Fig. 17 is obtained from the average of the corresponding heat transfer data before the separation bubble.

Discussion

Effect of Negative Jet. In the previous section some discussion was made about the asymmetric profiles of the Nusselt number around the semicircular leading edge at the lowest inlet Reynolds number condition, which was also observed in the study by O'Brien (1990). Meanwhile, O'Brien, along with Paxson and Mayle (1991), has claimed that so-called negative jet effects appeared around the leading edge under the influence of the periodic passing wakes and such effects were detected in different fashions on the leeward and windward side of the leading edge, which correspond to the right and left side, respectively, in the present notation. Consequently one might suppose that the above-mentioned asymmetric profiles were caused by those asymmetric effects of the wakes to some extent. Such supposition is partially supported by the author's previous experiments about the wake-affected heat transfer on a flat plate instead of the present test model as shown in the upper portion of Fig. 19 (Funazaki et al., 1993). This figure also illustrates the results obtained in those experiments, where the symbols with "R" represent the data in the reverse rotation case. It is found that the heat transfer coefficients for the reverse rotation are meaningfully lower than those of the normal rotation case, though the differences in magnitude are not as large as 10 percent of the normal rotation data. Accordingly it is concluded that the rotation direction of the disk in the wake generator might affect the heat transfer around the circular leading edge, but its effect is a somewhat limited one.

Comparison With O'Brien's Experiment. From his experiment using a spoked-wheel wake generator in an annular-flow wind tunnel, O'Brien (1990) measured the time-averaged

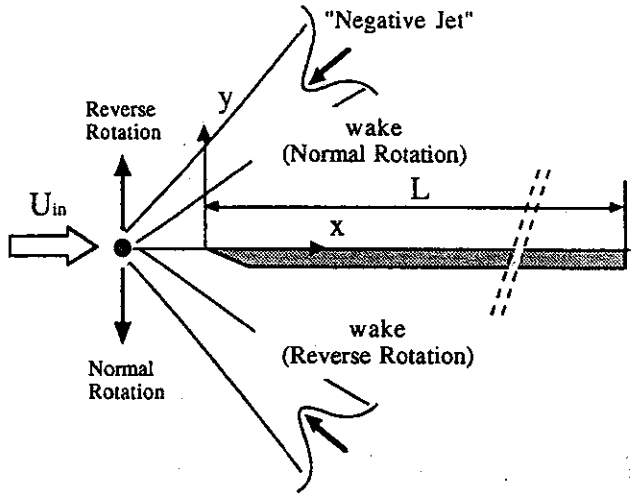

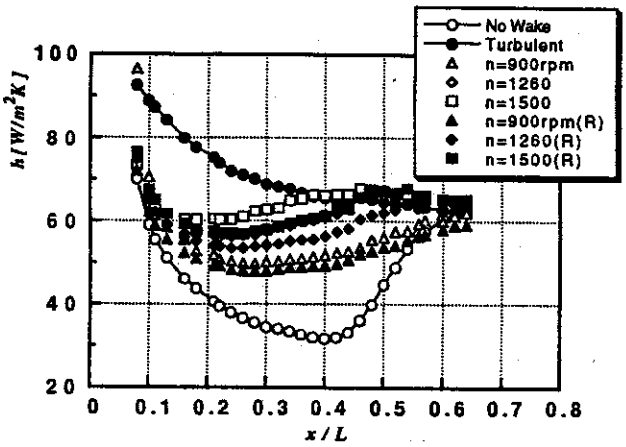

Fig. 19 Wake-affected heat transfer on the flat plate with the wake generator being rotated in the normal and the reverse directions (Funazaki et al., 1993)

heat transfer around the test cylinder with a 12.7 mm diameter; these results are shown in Fig. 21. In this figure, the ordinate is the ratio of wake-affected Nusselt number to the corresponding steady Nusselt number at the stagnation line against the Strouhal number. Note that the definition of Strouhal number in the O'Brien paper differs from the present definition, so that the data in Fig. 20 are reproduced from the original paper according to the present definition. Also shown in this figure is the correla-

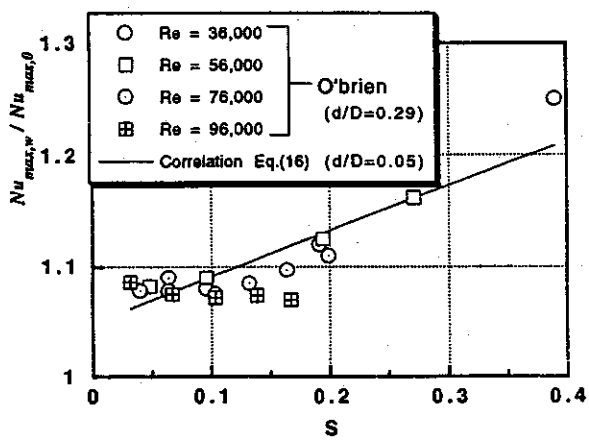

Fig. 20 Comparison between the present correlation (Eq. (15)) and the experimental data by O'Brien (1990)

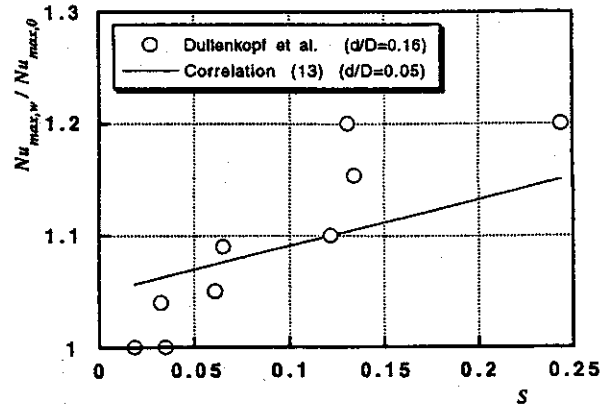

Fig. 21 Comparison between the present correlation (Eq. (16)) and the experimental data by Dullenkopf et al. (1990)

tion curve of Eq. (13), for comparison. The heat transfer ratio at the Strouhal number less than 0.1 is almost of constant value ($\cong$1.08), and at the higher Strouhal numbers the ratio tends to increase according to the Strouhal number in almost the same manner with the correlation. Agreement between the O'Brien data and the correlation at the higher Strouhal numbers surprising, considering the fact that the diameter ratios of wake-generating bar and test model (d/D) employed in the two studies are quite different, where $d/D = 0.29$ for the O'Brien's experiment and $d/D = 0.05$ for the present study.

Comparison With the Cascade Test Data. Dullenkopf et al. (1990) conducted an experiment similar to the present one using the linear cascade as well as the rotating wake generator. From the wake-affected heat transfer distributions around the blade leading edge in their paper, the heat transfer enhancement at the stagnation line, $Nu_{max,w}/Nu_{max,0}$, are calculated and compared with the correlation (Eq. (16)), as shown in Fig. 21. Consequently, it is found that the present correlation yields results similar to the data derived from the cascade test. However, some quantitative differences between the two appear in a meaningful fashion, which can probably be attributed to the uncertainties involved in both experiments.

Conclusions

The influence of the periodic passing wakes on the heat transfer over the leading edge as well as the flat plate was investigated. Local heat transfer distributions along the test surface were measured under the several unsteady conditions of the bar-passing Strouhal number for four inlet Reynolds numbers. The findings in this study are summarized as follows:

1 The heat transfer along the surface of the test model is enhanced by the periodic passing wakes from the moving bars, and such enhancing effect becomes prominent as the bar-passing Strouhal number increases.

2 In the lowest Reynolds number case, the profiles of the wake-affected heat transfer around the stagnation region become considerably asymmetric about the geometric stagnation line, especially at the higher Strouhal number. This is mainly because of the flow being turned by the moving bars ahead of the test model.

3 The dependency of the wake-affected Stanton number around the stagnation region on the local Reynolds number is quite similar to that of the no wake condition. This means the Stanton number in the region is proportional to $Re_x^{1/2}$. From this finding, a correlation is deduced for the enhancement factor due to the periodic wakes.

4 Comparisons are made between the correlations obtained in this study and the other experimental data, and it follows

that the present study yields similar results to those of the previous studies about the wake effect, despite the large difference in the geometric conditions.

Acknowledgments

The work reported in this paper is financially supported by Aero-engine Division of IHI, Ishikawajima-Harima Heavy Industries, under the supervision of S. Yamawaki. The author is greatly indebted to Freedrick P. Laing, a former student of Iwate University, for his valuable involvement in conducting the experiment, and to Y. Yamashita for his great help in manufacturing the test model.

References

Benedict, R. P., 1969, *Fundamental of Temperature, Pressure, and Flow Measurements*, Wiley, New York.

Dullenkopf, K., and Mayle, R. E., 1994, "The Effects of Incident Turbulence and Moving Wakes on Laminar Heat Transfer in Gas Turbines," ASME JOURNAL OF TURBOMACHINERY, Vol. 116, pp. 23–28.

Dullenkopf, K., Schulz, A., and Wittig, S., 1991, "The Effect of Incident Wake Conditions on the Mean Heat Transfer of an Airfoil," ASME JOURNAL OF TURBOMACHINERY, Vol. 113, pp. 412–418.

Frossling, N., 1958, "Evaporation Heat Transfer and Velocity Distribution in Two-Dimensional and Rotationally-Symmetric Laminar Boundary Layer," NACA TM-1432.

Funazaki, K., 1989, "Measuring Technique of Heat Transfer on Turbine Airfoils Using Boundary Element Method," *IHI Technical Report*, Vol. 28, pp. 327–332.

Funazaki, K., Meguro, T., and Yamawaki, S., 1993, "Studies on the Unsteady Boundary Layer on a Flat Plate Subjected to Incident Wakes (Forced Transition Models of the Boundary Layer)," *JSME International Journal*, Vol. 36, pp. 532–539.

Kays, W. M., and Crawford, M. E., 1980, *Convective Heat and Mass Transfer*, McGraw-Hill, New York, p. 140.

Kline, S. J., and McClintock, F. A., 1953, "Describing Uncertainties in Single Sample Experiments," *Mechanical Engineering*, Jan., pp. 3–8.

Lowry, G. W., and Vachon, R. I., 1975, "The Effect of Turbulence on Heat Transfer From Heated Cylinders," *International Journal of Heat and Mass Transfer*, Vol. 18, pp. 1229–1242.

Magari, P. J., and Lagraff, L. E., 1994, "Wake-Induced Unsteady Stagnation-Region Heat Transfer Measurements," ASME JOURNAL OF TURBOMACHINERY, Vol. 116, pp. 29–38.

Mehendale, A. B., Han, J. C., and Ou, S., 1991, "Influence of High Mainstream Turbulence on Leading Edge Heat Transfer," ASME *Journal of Heat Transfer*, Vol. 113, pp. 843–850.

O'Brien, J. E., 1990, "Effects of Wake Passing on Stagnation Region Heat Transfer," ASME JOURNAL OF TURBOMACHINERY, Vol. 112, pp. 522–530.

Paxson, D. E., and Mayle, R. E., 1991, "Laminar Boundary Layer Interaction With an Unsteady Passing Wake," ASME JOURNAL OF TURBOMACHINERY, Vol. 113, pp. 419–427.

Yoshida, T., 1993, "Progress in High Temperature Turbine Cooling Technology and Its Prospects," *Journal of the Gas Turbine Society of Japan*, Vol. 20, pp. 4–9.

DISCUSSION

R. E. Mayle[1] and K. Dullenkopf[2]

Even the simplest physical consideration concerning the effect of passing wakes in the free stream on heat transfer indicates that the correlations given in Eqs. (15) and (16) cannot be generally valid. In particular, neither correlation contains any quantity related to the individual wakes. To illustrate the wake's role, if Nu_0 is the Nusselt number for a position on the surface without passing wakes and Nu_w is a representative Nusselt number in the wake, then the time-averaged Nusselt number for a flow with periodically passing wakes is $\overline{Nu} = Nu_0 + (Nu_w - Nu_0)(\tau_w/\tau)$, where τ_w is a representative passing time for the wake over any point on the surface and τ is the period between wakes. For no wake, $\tau_w = 0$, or no augmentation caused by the wake, $Nu_w = Nu_0$, the time-averaged Nusselt number is, as expected, Nu_0. For a completely wake saturated flow, $\tau_w = \tau$, and $\overline{Nu} = Nu_w$ as expected.

Introducing your definition of the Strouhal number, $S = fD/U_{in}$, the above expression becomes $\overline{Nu} = Nu_0 + (Nu_w - Nu_0) \times (U_{in}\tau_w/D)S$, which clearly indicates that the coefficient of the Strouhal number (which you consider constant in Eqs. (15) and (16)) really depends on wake-related quantities. Such quantities are wake turbulence level and length scales, which affect Nu_w, and the wake width, which affect τ_w. Since different experiments have different wake characteristics, wake passing times, and periods, all which affect the coefficient of S in this simplest of models, the poor comparisons shown in Figs. 20 and 21 should not be surprising. For details regarding a more realistic model for the effect of passing wakes on laminar heat transfer, you are referred to Dullenkopf and Mayle (1994).

Author's Closure

The author would like to acknowledge the comment from Mayle and Dullenkopf. As described in their comment or in their paper (Dullenkopf and Mayle, 1992), it is necessary to take account of several factors of the wake characteristics in order to gain a thorough understanding of how the wake passage affects the heat transfer around stagnation regions. In particular, much attention must be paid to wake structure and its turbulence length. The author also agrees with the viewpoint of Dullenkopf and Mayle, which implies that wakes at higher turbulence levels would produce heat transfer enhancement, almost independent of the wake generation. The author believes this could be applied to the present case.

Although Dullenkopf and Mayle (1992) proposed a simple but useful method for predicting wake-affected heat transfer around the stagnation region, the author has not been fully contented with their method because there was no information given to evaluate the Nusselt number Nu_w or the wake duration τ_w. This situation directed the author to start the present study. Since effects of free turbulence are not included in his experiment, this paper does not provide a general correlation on the wake-affected heat transfer for the readers. Therefore, the author has proceeded with his research to investigate effects of free-stream turbulence upon the wake-affected heat transfer, which also discusses how Nu_w or τ_w should be specified (Funazaki, 1994; Funazaki et al., 1995). Despite this study, much remains to be done for further understanding of this complicated phenomenon.

References

Funazaki, K., 1995, "Studies on Wake-Affected Heat Transfer Around the Leading Edge of Turbine Blades (Modeling of Heat Transfer Enhancement)," *Journal of the Gas Turbine Society of Japan*, Vol. 22, pp. 83–90.

Funazaki, K., et al., 1995, "Studies on Wake-Affected Heat Transfer Around the Leading Edge of a Blunt Body," *Proc. ASME/JSME Thermal Engineering Conference*, Vol. 1, pp. 343–350.

[1] Professor Emeritus of Mechanical Engineering, Rensselaer Polytechnic Institute, Troy, NY 12180 USA.

[2] Dr.-Ingenieur, Institut für Thermische Strömungs Maschinen, Universität Karlsruhe, 76128 Karlsruhe, Germany.